1-1-1990

Extended x-ray-absorption fine-structure studies of Zn1-xMnxSe alloy structure

Way Faung Pong

Robert A. Mayanovic

Bruce A. Bunker

J. K. Furdyna

U. Debska

Recommended Citation

Pong, W-F., Robert A. Mayanovic, Bruce A. Bunker, J. K. Furdyna, and U. Debska. "Extended x-ray-absorption fine-structure studies of Zn 1− x Mn x Se alloy structure." Physical Review B 41, no. 12 (1990): 8440.

Extended x-ray-absorption fine-structure studies of $Zn_{1-x}Mn_xSe$ alloy structure

W.-F. Pong, R. A. Mayanovic, B. A. Bunker, J. K. Furdyna, and U. Debska
Department of Physics, University of Notre Dame, Notre Dame, Indiana 46556
(Received 7 November 1989)

Bond lengths, Debye-Waller factors, and site occupancy in the diluted magnetic semiconductor $Zn_{1-x}Mn_xSe$ have been measured using extended x-ray-absorption fine structure. The nearest-neighbor bond lengths at both room temperature and low temperature (77 K) are found to be constant as a function of alloy composition within the experimental uncertainty of 0.01 Å. Because the average cation-cation distance changes with Mn content, these results necessarily imply distortion of the tetrahedral bond angles. The anion sublattice is shown to suffer the largest distortion, but the cation sublattice also exhibits some relaxation. The repercussions of these results are discussed, in terms of the amount of cation and anion sublattice distortion at low temperature and its connection to the superexchange mechanism occurring between the Mn^{2+} ions and mediated by the intervening anion in $Zn_{1-x}Mn_xSe$.

I. INTRODUCTION

The ternary alloys $A^{II}_{1-x}Mn_xC^{VI}$ (A^{II}=Zn,Cd,Hg; C^{VI}=S,Se,Te), belong to a group of materials known as diluted magnetic semiconductors (DMS's), where the group-II cations A^{II} are randomly replaced in part by substitutional magnetic Mn^{2+} ions. Extensive studies[1] have revealed that DMS's exhibit unique electrical, magnetic, and optical properties,[2] attributed to the short-ranged exchange interactions between the spins of the Mn^{2+} ions and between the Mn^{2+} ions and the band electrons.

The lattice parameters of $A^{II}_{1-x}Mn_xC^{VI}$ type DMS's have been deduced by Yoder-Short *et al.*[3] using x-ray diffraction. They found that the mean cation-cation distance (d_c) varies linearly with Mn concentration x and obeys Vegard's law. It is not clear from this study, however, how the local cation-anion, cation-cation, and anion-anion distances vary with x. The purpose of this paper is to report on our study of the local structure of the Mn^{2+} ion in the A^{II}-C^{VI} host lattice: The variation of the cation-anion, the cation-cation, and anion-anion distances with x in terms of the degree of the cation sublattice and anion sublattice distortion and its connection to the superexchange mechanism occurring between the Mn^{2+} ions and mediated by the intervening anion in $Zn_{1-x}Mn_xSe$. We also discuss our results concerning the fluctuation in these distances throughout the sample, in terms of the Debye-Waller factor, and on possible "site correlation" in the alloy.

Extended x-ray-absorption fine structure (EXAFS) is an ideal structural probe for disordered systems such as random alloys. In particular, the technique has been used in determination of the distortions of the host lattice in the vicinity of impurities in dilute binary alloys[4] as well as the near-neighbor environment in ternary[5–7] and quaternary[8,9] solid solutions.

II. MEASUREMENTS AND ANALYSIS

We have performed EXAFS measurements on three $Zn_{1-x}Mn_xSe$ samples having x=0.15,0.35,0.57. The samples were grown using Bridgman's technique[10] and characterized with x-ray diffraction. The EXAFS spectra were obtained in transmission mode at the National Synchrotron Light Source (NSLS), using the X11A beamline. The sample measurements included the cation Zn, Mn, and anion Se K edges of $Zn_{1-x}Mn_xSe$ alloys, and both ZnSe and MnSe binary compounds. Measurements were obtained at both room temperature and 77 K. We have analyzed the Zn, Mn, and Se K edges in order to determine the nearest-neighbor (NN) Zn—Se, Mn—Se bond lengths and next-nearest-neighbor (NNN) cation-cation, anion-anion distances in $Zn_{1-x}Mn_xSe$.

EXAFS data analysis, including Fourier isolation of the first- and second-shell data for $Zn_{1-x}Mn_xSe$ was done using procedures described elsewhere.[11] The normalized EXAFS oscillations for both Zn and Mn K edge of $Zn_{0.85}Mn_{0.15}Se$ are shown in Fig. 1; the corresponding Fourier transforms are shown in Fig. 2. Further analysis first involved use of the "ratio method,"[11] where the alloy data were compared with spectra from ZnSe and MnSe for determining the NN bond lengths, and second, use of nonlinear least-squares fitting to analyze the NNN data. The ratio method was used to obtain the Mn—Se and Zn—Se bond lengths in $Zn_{1-x}Mn_xSe$ from the Mn and Zn K-edge EXAFS data, measured at room temperature and 77 K. Because the Debye-Waller factors in the EXAFS spectra are related to the mean-square fluctuations in interatomic distances, the EXAFS Debye-Waller factor σ^2 is the sum of a static and thermal component $\sigma^2(T)=\sigma_s^2+\sigma_{th}^2(T)$, where "$s$" and "th" subscripts represent the static and thermal parts, respectively. The structural disorder σ_s^2 is essentially temperature independent, while $\sigma_{th}^2(T)$ arises from temperature-dependent

thermal vibrations. The NNN distances correspond to the second main peak in the Fourier transform of the EXAFS spectrum. The Debye-Waller factor associated with the second shell substantially reduces the amplitude of the EXAFS oscillations measured at room temperature, making it difficult to obtain the NNN distances in $Zn_{1-x}Mn_xSe$ at 300 K. Lowering the temperature significantly reduced the Debye-Waller thermal disorder factor thereby enhancing the EXAFS oscillation amplitude and signal to noise ratio. A comparison of Fig. 3 to Fig. 2 shows the second peak in the Fourier transform of the EXAFS signal becoming much more prominent at 77 K for both the Zn edge and Mn edge. We were able to accurately analyze the low-temperature (77 K) second-shell EXAFS data of $Zn_{1-x}Mn_xSe$, using the nonlinear least-squares-fit method, and have obtained from this analysis the NNN cation-cation and anion-anion distances.

ZnSe and MnSe lattice constants at 77 K were obtained from the room-temperature lattice constants [5.668 Å for ZnSe and 5.461 Å for MnSe (NaCl structure)] as determined by x-ray diffraction measurements, and $\bar{\alpha}$, the average thermal expansion coefficient over the temperature range. The values for $\bar{\alpha}$ used were $\sim 1.2\times10^{-5}$ K^{-1} for ZnSe and $\sim 2.9\times10^{-5}$ K^{-1} for MnSe having the NaCl structure. These values of $\bar{\alpha}$ were calculated from low-temperature x-ray diffraction measurements revealing the lattice constant of ZnSe to contract by 0.003 Å between room temperature and 52.4 K, and the lattice constant of MnSe to contract by 0.008 Å between room temperature and 27.3 K.

Figure 4 shows the normalized Se K-edge EXAFS oscillations and the corresponding Fourier transforms for $Zn_{0.85}Mn_{0.15}Se$ measured at 77 K. There are 12 NNN Se atoms surrounding the central Se atom, in both the zinc-blende and wurtzite structures, that contribute to the Se K-edge EXAFS signal. Since, for any one x, the NN Zn—Se tetrahedral bond length $d_{\text{Zn-Se}}$ is shorter than the NN Mn—Se tetrahedral bond length $d_{\text{Mn-Se}}$, it is apparent that if the tetrahedral bond angles are fairly close to one another irrespective of the atomic arrangement, then the NNN distance $d_{\text{Se-Zn-Se}}$ will be shorter than $d_{\text{Se-Mn-Se}}$, where $d_{\text{Se-Zn-Se}}$ is the distance from the central Se atom to a NNN Se atom with a Zn atom intervening between the Se atoms and likewise $d_{\text{Se-Mn-Se}}$ is the corresponding Se-Se distance with a Mn atom acting as the in-

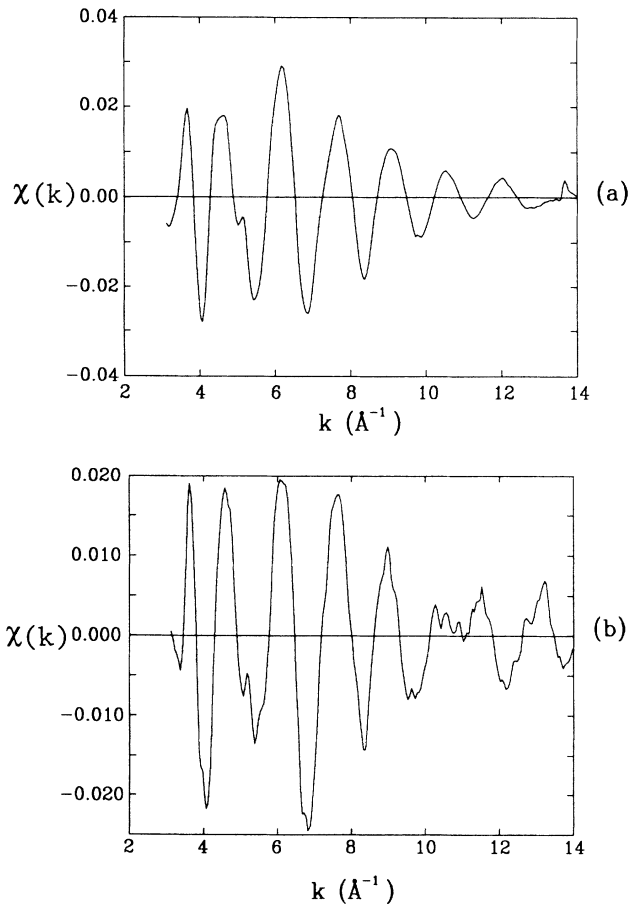

FIG. 1. Normalized EXAFS oscillations for (a) the Zn K edge and (b) Mn K edge of $Zn_{0.85}Mn_{0.15}Se$. All data were obtained at room temperature.

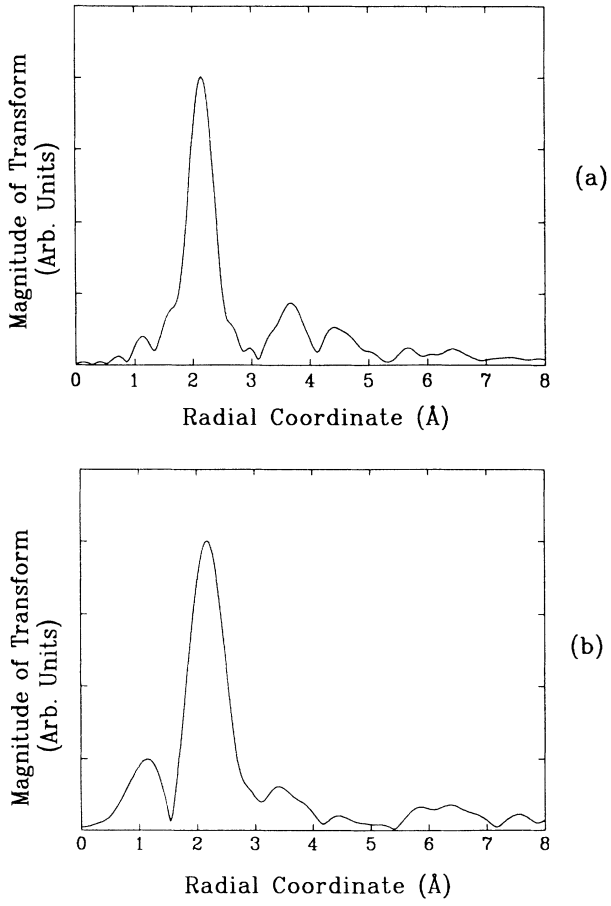

FIG. 2. Magnitude of Fourier transform of (a) the Zn K edge and (b) Mn K edge of $Zn_{0.85}Mn_{0.15}Se$. All data were obtained at room temperature.

tervening atom. Because interference between the peaks occurs in the Se K-edge EXAFS spectrum and $d_{\text{Se-Zn-Se}}$, $d_{\text{Se-Mn-Se}}$ distances are too close to separate using the ratio method we chose instead to analyze the data using nonlinear least-squares fitting. The standard $d_{\text{Se-Zn-Se}}$ and $d_{\text{Se-Mn-Se}}$ data used with this technique to analyze the alloy samples were taken from the Se K-edge data of ZnSe and MnSe, respectively.

In contrast, the analysis of the Zn and Mn K-edge NNN EXAFS data, for the purpose of obtaining $d_{\text{cation-cation}}$, is more complicated by the lack of experimental standard for the Zn-edge $d_{\text{Zn-Mn}}$ data and Mn-edge $d_{\text{Mn-Zn}}$ data. Teo and Lee[12] have tabulated theoretical phase shifts and backscattering amplitudes which may be used to generate Zn-edge $d_{\text{Zn-Mn}}$ and Mn-edge $d_{\text{Mn-Zn}}$ data for use as standards. While these calculations are very useful, it is well known that they are not accurate enough to use directly for precise results. To overcome these difficulties, we have used a combination of experimental phases and amplitudes and *changes* in the theoretical results with atomic number. In the Zn-edge case, we have, schematically,

$$\phi_{\text{Zn-Mn}} \approx \phi^{\text{expt}}_{\text{Zn-Zn}} + (\phi^{\text{theory}}_{\text{Zn-Mn}} - \phi^{\text{theory}}_{\text{Zn-Zn}})$$

and

$$A_{\text{Zn-Mn}} \approx A^{\text{expt}}_{\text{Zn-Zn}} (A^{\text{theory}}_{\text{Zn-Mn}} / A^{\text{theory}}_{\text{Zn-Zn}}) ,$$

where ϕ and A are, respectively, the phase and amplitude terms in the EXAFS χ data. We believe this method is much more accurate than one which depends solely on theoretical calculations.

A comment on the analysis of EXAFS data: The fitting processes which we used above included eight adjustable parameters (N, coordination number; R, radial distance; $\Delta\sigma^2$, relative Debye-Waller factor; ΔE_0, relative edge energy, for each single shell), but typically four parameters can be varied at one time.

III. EXPERIMENTAL RESULTS

The results of the analysis for the first-shell NN bond lengths (ratio method) at room temperature and 77 K in $Zn_{1-x}Mn_xSe$ are summarized in Figs. 5 and 6. Although x-ray diffraction measurements show the mean cation-cation distance to increase linearly with x by approximately 0.1 Å through the series, and the crystal structure to change from cubic (zinc blende) to hexagonal (wurt-

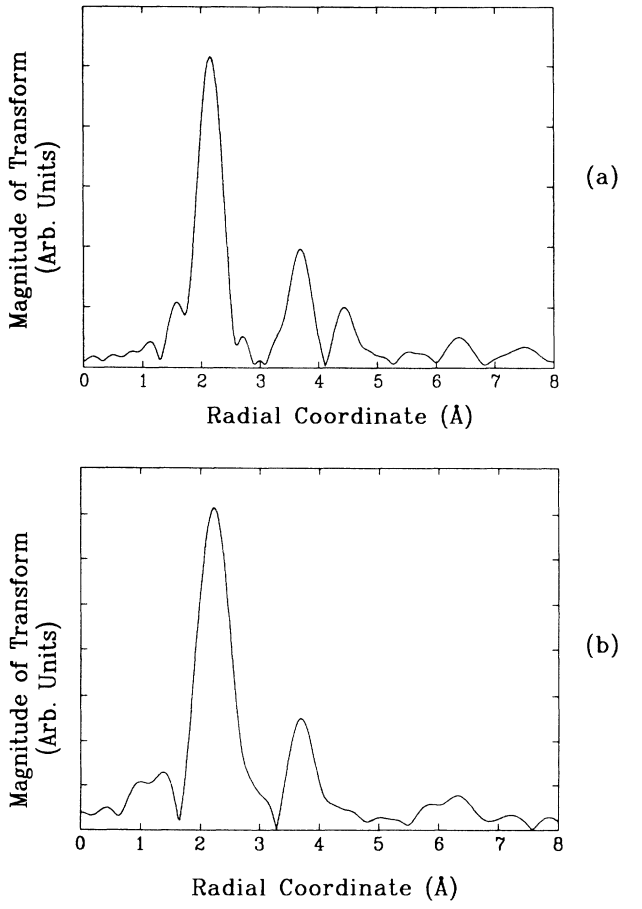

FIG. 3. Magnitude of Fourier transform of (a) the Zn K edge and (b) Mn K edge of $Zn_{0.85}Mn_{0.15}Se$. All data were obtained at 77 K.

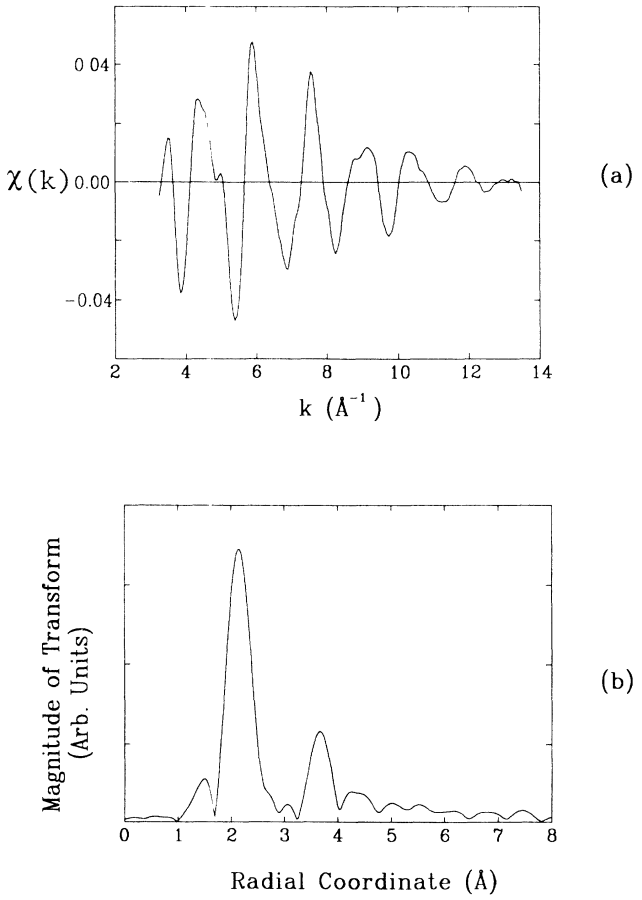

FIG. 4. (a) Normalized EXAFS oscillations for the Se K edge and (b) magnitude of Fourier transform of the Se K edge of $Zn_{0.85}Mn_{0.15}Se$. All data were obtained at 77 K.

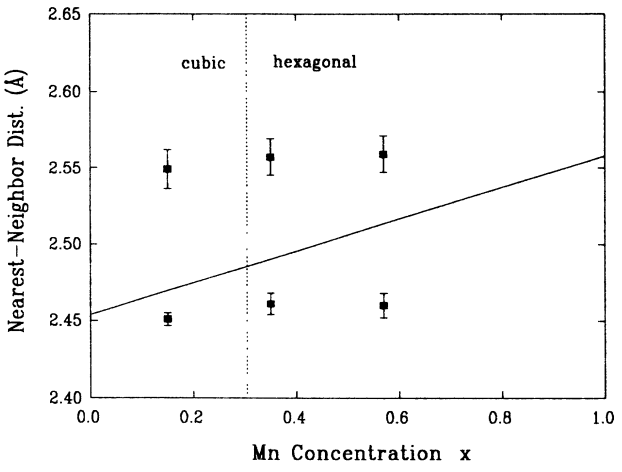

FIG. 5. EXAFS results for Zn—Se bond distances (lower solid squares), Mn—Se bond distances (upper solid squares), and a linear fit to the x-ray diffraction cation-cation distance results, multiplied by a $\sqrt{3/8}$ factor, taken from Ref. 3 (solid line). All data were obtained at room temperature.

zite) as a function of Mn concentration with the transition at $x \sim 0.3$, the NN bond lengths show no change within the experimental uncertainty of 0.01 Å at both room temperature and 77 K.

Furthermore, the first-shell results at room temperature show that the sample with $x = 0.35$ has a larger relative Debye-Waller factor $\Delta\sigma^2 = \sigma^2_{\text{sample}} - \sigma^2_{\text{standard}}$, for both the Zn-edge and Mn-edge results, than samples having $x = 0.15$ and 0.57. These results are shown in Fig. 7. The Debye-Waller factors ($\Delta\sigma^2$) in Fig. 7(b), pertaining to the Mn—Se bond, have negative values because the Mn—Se bond lengths in the NaCl-structured MnSe standard have a larger σ^2 than those in tetrahedrally bonded $Zn_{1-x}Mn_xSe$. In view of the fact that the phenomenon persists at 77 K where the σ^2_{th} is reduced considerably (we estimate $\sigma^2_s \approx \sigma^2_{\text{th}}$ in magnitude for $Zn_{1-x}Mn_xSe$ at this temperature), the increased $\Delta\sigma^2$ for $x = 0.35$ we believe is

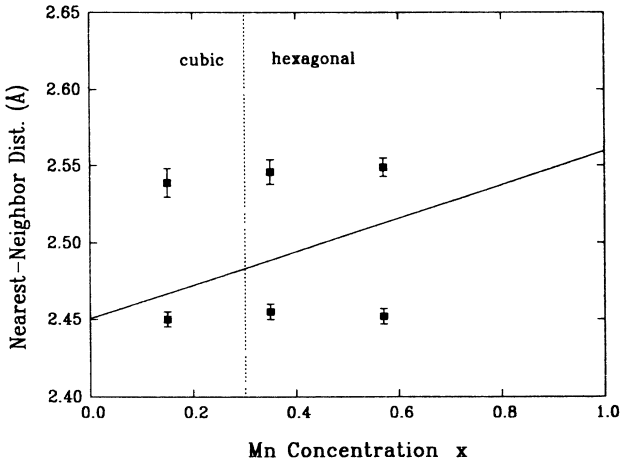

FIG. 6. EXAFS results for Zn—Se bond distances (lower solid squares), Mn—Se bond distances (upper solid squares), and a linear fit to VCA results (solid line). All data were obtained at 77 K.

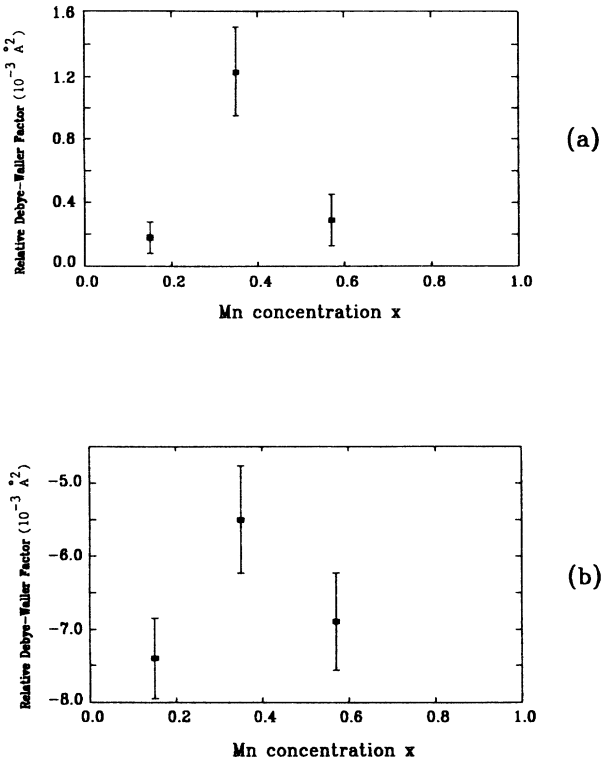

FIG. 7. (a) The Zn K-edge Debye-Waller factor values for $Zn_{1-x}Mn_xSe$ alloys relative to the value for the ZnSe standard and (b) the Mn K-edge Debye-Waller factor values for $Zn_{1-x}Mn_xSe$ alloys relative to the value for the MnSe standard, obtained from data measured at room temperature.

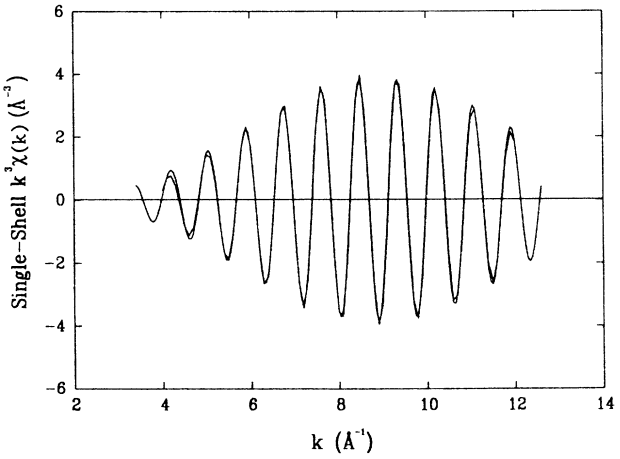

FIG. 8. The experimental filtered $k^3\chi(k)$ (solid line) and the nonlinear least-squares-fitting data (dashed line) of $Zn_{0.85}Mn_{0.15}Se$, for the Se K edge measured at 77 K.

due to a larger static structural disorder occurring near the structural phase transition between the zinc-blende and wurtzite phases. The first-shell data of the system $Hg_{1-x}Mn_xTe$,[13] which has a single zinc-blende structural phase up to $x \sim 0.75$, does *not* show a substantial increased $\Delta\sigma^2$ for any one sample.

Figure 8 shows the experimental and fitted low-temperature $k^3\chi$ data, of $Zn_{0.85}Mn_{0.15}Se$, obtained from the second-shell contribution to the Se K-edge EXAFS signal. The resulting anion-anion NNN distances $d_{\text{Se-Zn-Se}}$ and $d_{\text{Se-Mn-Se}}$ are shown in Fig. 9. The solid line in Fig. 9 represents the anion-anion NNN distances in the virtual-crystal approximation (VCA): It is a weighted mean of both $d_{\text{Se-Zn-Se}}$ and $d_{\text{Se-Mn-Se}}$, calculated using $d_{\text{Se-Se}}^{\text{VCA}} = (1-\bar{x})d_{\text{Se-Zn-Se}} + \bar{x}d_{\text{Se-Mn-Se}}$, where $\bar{x}$ in this case refers to a fractional value of the coordination number of Mn atoms deduced experimentally from fitting results for each sample. As shown in Fig. 9, both anion-anion NNN distances vary slightly with Mn content, particularly the $d_{\text{Se-Mn-Se}}$ distances. This implies that the anion sublattice undergoes considerable distortion away from the VCA.

We have successfully analyzed, using the nonlinear least-squares-fitting technique, the low-temperature (77 K) Zn and Mn K-edge data for our $Zn_{1-x}Mn_xSe$ samples. The Zn and Mn K-edge filtered χ data and our fitting results for the data, for $Zn_{0.85}Mn_{0.15}Se$, are shown in Fig. 10. The $Zn_{1-x}Mn_xSe$ cation-cation NNN distances are plotted as a function of Mn concentration in Fig. 11. The VCA for $d_{\text{cation-cation}}$ in Fig. 11, which is a weighted mean of the NNN distances $d_{\text{Zn-Se-Zn}}$, $d_{\text{Zn-Se-Mn}}$ (or $d_{\text{Mn-Se-Zn}}$), and $d_{\text{Mn-Se-Mn}}$, is computed using

$$d_{\text{cation-cation}}^{\text{VCA}} = (1-\bar{x})^2 d_{\text{Zn-Se-Zn}} + 2\bar{x}(1-\bar{x})d_{\text{Zn-Se-Mn}} + \bar{x}^2 d_{\text{Mn-Se-Mn}} .$$

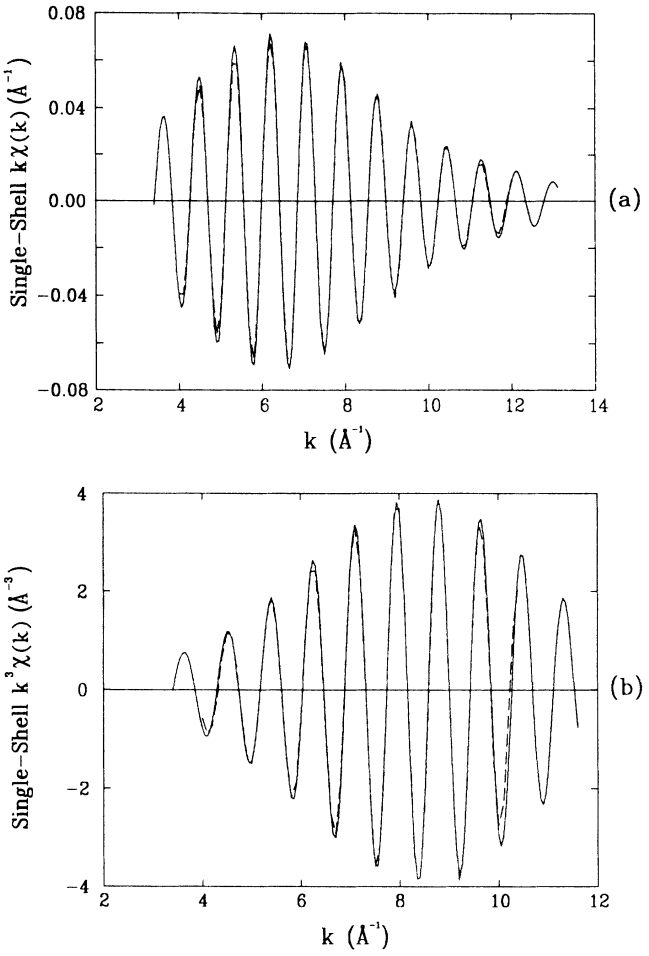

FIG. 10. (a) Filtered Zn K-edge $k\chi(k)$ data (solid line) and the nonlinear least-squares fit (dashed line). (b) Filtered Mn K-edge $k^3\chi(k)$ data (solid line) and the nonlinear least-squares fit (dashed line). Both (a) and (b) are for $Zn_{0.85}Mn_{0.15}Se$ and data measured at 77 K.

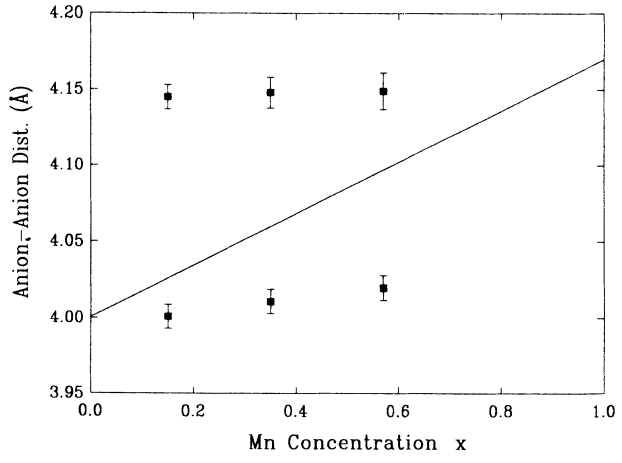

FIG. 9. EXAFS results from the Se K edge of $Zn_{1-x}Mn_xSe$ measured at 77 K for $d_{\text{Se-Mn-Se}}$ distances (upper solid squares) and $d_{\text{Se-Zn-Se}}$ distances (lower solid squares); the solid line represents the VCA linear fit to the anion-anion distances.

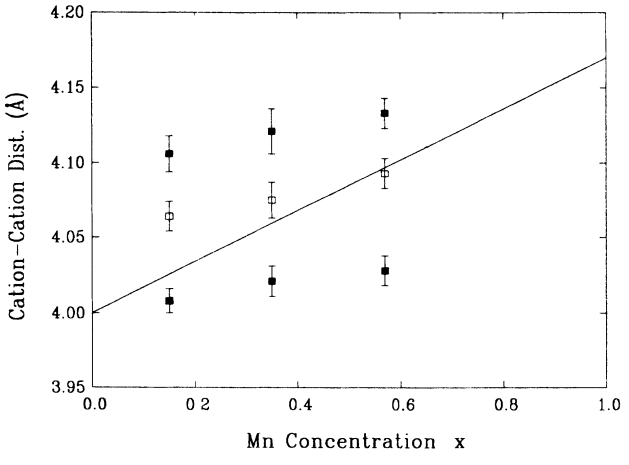

FIG. 11. Low-temperature (77 K), EXAFS results for the cation-cation distances $d_{\text{Mn-Se-Mn}}$ (upper solid squares), $d_{\text{Zn-Se-Mn}}$ (open squares), and $d_{\text{Zn-Se-Zn}}$ (lower solid squares). The solid line is a linear fit to the VCA of the cation-cation distances.

These results show that the cation-cation NNN distances vary substantially with x, and in particular approach their respective VCA values considerably more than do the anion-anion NNN distances in comparison to their VCA values. However, the fact that the $d_{\text{cation-cation}}$ deviate considerably from $d^{\text{VCA}}_{\text{cation-cation}}$ distances indicates that the cation sublattice *also* experiences an appreciable amount of distortion. As in the case for the NNN anion-anion distances, the error bars associated with NNN cation-cation distances may be slightly underestimated because the $\Delta\sigma^2$'s for the alloys are indicative of a larger range of distance distributions; in this case the largest $\Delta\sigma^2$'s are ~ 0.008 Å^2 for the Zn edge and ~ 0.057 Å^2 for the Mn edge.

From our fitting results of the anion-anion and cation-cation NNN data for the $Zn_{1-x}Mn_xSe$ alloys, taken at 77 K, we have obtained the average Mn and Zn atom coordination number values in the second shell; the results from the Zn K-edge data are shown in Fig. 12. If the Mn and Zn atoms were totally randomly distributed, the number of Mn and Zn atoms in the second shell, about a Zn site, would be proportional to x and $1-x$, respectively. On the other hand, if the Mn and Zn atoms tended to cluster in the alloys, then we would expect to see a larger Zn-Zn coordination number than that obtained in the randomly distributed case. The results of this work show a slight but consistent deviation from the random second-shell distribution; the Zn-Mn atom coordination numbers in $Zn_{1-x}Mn_xSe$ are slightly larger than expected from the random distribution, and Zn-Zn atom coordination numbers are slightly *smaller* than expected. These results are therefore inconsistent with clustering, and may actually indicate a tendency for *ordering* in $Zn_{1-x}Mn_xSe$ alloys.

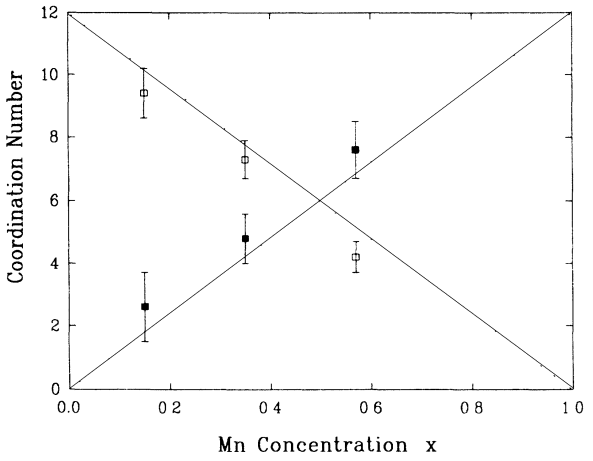

FIG. 12. The average values for the Zn (open squares) and Mn atom (solid squares) coordination numbers obtained from the Zn K edge, measured at 77 K, as a function of Mn concentration. The dashed lines represent the corresponding Zn and Mn atom second-shell coordination number values as a function of x based on the random distribution model.

IV. INTERPRETATION

Our results show evidence for the distorted configuration of the anion relative to the nearest-neighboring cations in $Zn_{1-x}Mn_xSe$, because the NN bond lengths in the alloys are approximately independent of x while the mean cation-cation distance obeys Vegard's law. This indicates that the alloy structure is close to Bragg's and Pauling's concept.[14] Furthermore, based on our results for $Zn_{1-x}Mn_xSe$ and bond length results obtained from EXAFS measurements made previously on $Cd_{1-x}Mn_xTe$,[6] $Hg_{1-x}Mn_xTe$,[13] and $Zn_{1-x}Mn_xS$,[15] it appears that a general trend is emerging. Namely, the A^{II}-C^{VI} and (Mn^{2+})—C^{VI}NN bond lengths are almost independent of x. Balzarotti *et al.*[6] have been able to show that their model of the microscopic structure of $A_{1-x}B_xC$ ternary alloys, having the zinc-blende structure, describes the NN cation-anion bond length results of $Cd_{1-x}Mn_xTe$. In their model they assume a random cation distribution and a cation sublattice that remains undistorted. The anion sublattice is assumed to distort, in accordance with the above-mentioned assumptions, as x is varied.

Although our results for the NNN distances in $Zn_{1-x}Mn_xSe$ alloys show that the cation sublattice distorts less than the anion sublattice, we find appreciable distortion in both sublattices. We should note that preliminary x-ray standing wave experiments on $Cd_{1-x}Mn_xTe$, performed by Durbin,[16] reveal that both the cation and anion sublattices distort as a result of Mn^{2+} cation substitution. We believe that a model capable of explaining these results has to take into account both the tetrahedral bond bending and bond stretching forces and the fact that NNN and perhaps even longer-range forces play a substantial role in determining the microstructural arrangement of the constituent atoms in DMS alloys.

Since the predominant type of exchange mechanism between Mn^{2+} ions in DMS is via the intervening anion in the form of superexchange, as first shown theoretically by Larson *et al.*,[17] it is important to understand the nature of the microscopic distortion of the local structure of DMS. The importance stems from the superexchange integral J_{dd} as calculated by Larson *et al.*,[17] being proportional to V_{do}^4, where V_{do} is the hybridization energy of the outermost Mn-d and anion-p orbitals, and therefore sensitive to the configuration of Mn^{2+} ions relative to each other and the anions in DMS. Besides also calculating an expression for the superexchange integral, Spalek *et al.*[18] showed that the amount of distortion from the ideal of an anion-centered tetrahedron in a DMS (both wide gap and narrow gap), resulting from substitution of Mn^{2+} ions for the A^{II} cations, is directly proportional to the experimental value of the exchange integral J (obtained from their susceptibility data) for that compound. Since the superexchange integral is theoretically dependent on the amount of distortion of the tetrahedron, this was experimental evidence in favor of superexchange being the predominant type of exchange mechanism in DMS. Our results support this idea and provide preliminary evidence that this is the case in narrow gap as well as wide

gap DMS's.[19]

There is a problem however, reconciling the model of Balzarotti *et al.*, which we use in this case for its simplicity, with the initial idea that J_{dd}, as predicted by Larson *et al.*,[17] is independent of x in the DMS ternary alloy system. As illustrated in Fig. 13, if the cation sublattice remains undistorted and the A^{II}-C^{VI} and Mn^{2+}-C^{VI} distances are independent of x then the anion shifts away from the center of the ideal tetrahedron, having four cations at its corners, either towards or away from the substituting Mn^{2+} ions depending on whether the host cation has a larger or smaller tetrahedral radius, respectively, than the Mn^{2+} ion. In this way the (Mn^{2+})—C^{VI}—(Mn^{2+}) bond angle θ is distorted away from the ideal tetrahedral bond angle by a small amount. As shown by Spalek *et al.*, $\Delta J_{dd} \propto \Delta\theta$, which implies that J_{dd} is *not* independent of x: While the (Mn^{2+})-C^{VI} distances remain constant with x, the Mn^{2+}-Mn^{2+} distance is expected to obey Vegard's law in the cation sublattice and thus $\Delta\theta$ is expected to depend on x, i.e., the average superexchange integral will depend on x—especially for higher concentrations.

A direct means of determining whether the superexchange integral is dependent on x in DMS is to deduce from the NN and NNN shell peak of the EXAFS data how the A^{II}-A^{II} and Mn^{2+}-Mn^{2+} distances vary with x. In fact, according to our EXAFS experimental results for both the NN ($d_{Zn\text{-}Se}$, $d_{Mn\text{-}Se}$) and the NNN ($d_{Zn\text{-}Zn}$, $d_{Mn\text{-}Mn}$) distances at 77 K, computing the bond angle from the geometrical point of view shown in Fig. 13, we find that the superexchange integral is fairly dependent on Mn concentration x because the Mn^{2+}—Se^{2-}—Mn^{2+} (also, Zn^{2+}—Se^{2-}—Zn^{2+}) bond angle varies with x. Figure 14 shows the amount of tetrahedral bond angle distortion, relative to the ideal tetrahedral bond angle ($\theta = 109.6°$), for both the Mn^{2+}—Se^{2-}—Mn^{2+} and Zn^{2+}—Se^{2-}—Zn^{2+} angles as a function of x. The overall linear behavior of the bond angles with x can be explained as follows: because the Mn^{2+} ion has a larger tetrahedral radius than the Zn^{2+} ion, upon substitution of Mn^{2+} for Zn^{2+} in the anion-centered tetrahedron, the Se^{2-} anion will be displaced away from the Mn^{2+} ions and toward the Zn^{2+} ions relative to its original position. Constraining the NN and NNN distances according to our results, i.e., the NN bond lengths remaining essentially constant, the anion sublattice distorting appreciably, and the cation sublattice also distorting but to a lesser degree, implies that the Mn^{2+}—Se^{2-}—Mn^{2+} bond angle will decrease slightly and the Zn^{2+}—Se^{2-}—Zn^{2+} increase slightly relative to 109.6°. In the small x limit, substitution of Mn^{2+} ions for Zn^{2+} ions results in the largest distortion of the Mn^{2+}—Se^{2-}—Mn^{2+} bond angle because the cation sublattice distorts less than the anion sublattice so that the Mn^{2+} ions occupy lattice sites close to those of Zn^{2+} ions but considerably different than the cation sites in the MnSe (hypothetical tetrahedrally bonded) binary compound. In the large x limit, the Mn^{2+} ions occupy cation sites considerably closer to those of the hypothetical wurtzite-structured MnSe compound resulting in appreciably less distortion of the Mn^{2+}—Se^{2-}—Mn^{2+} bond angle. The case for Zn^{2+}—Se^{2-}—Zn^{2+} bond angle is obviously reversed. As shown in Fig. 14, the extrapolation through the data points (dashed line) basically agrees with the ideal case where the Mn^{2+}—Se^{2-}—Mn^{2+} bond angle distortion goes to 0 at $x = 1$ and Zn^{2+}—Se^{2-}—Zn^{2+} bond angle distortion goes to 0 at $x = 0$.

According to Spalek *et al.*[18] the change in the superexchange integral ΔJ_{dd} is proportional to $\Delta a / a_{MnSe}$, where Δa is the difference between the cation-cation distance of the two binary compounds ZnSe ($x = 0$) and the hypothetical compound MnSe ($x = 1$), and a_{MnSe} is the Mn^{2+}-Mn^{2+} distance in MnSe. From their data, the largest distortion of the Mn^{2+}—Se^{2-}—Mn^{2+} bond angle

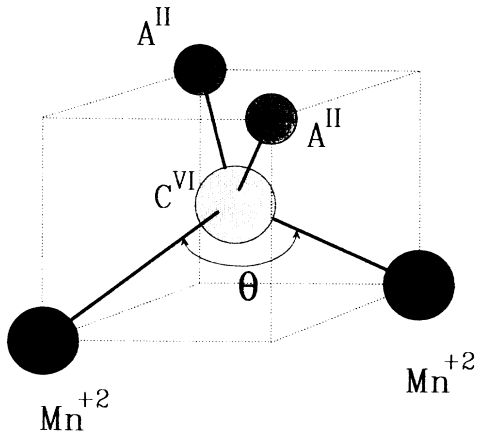

FIG. 13. Schematic of the distorted tetrahedral coordination about a Se atom, showing the bond angle θ. The magnetic interaction between the Mn^{2+} NNN is sensitive to this bond angle.

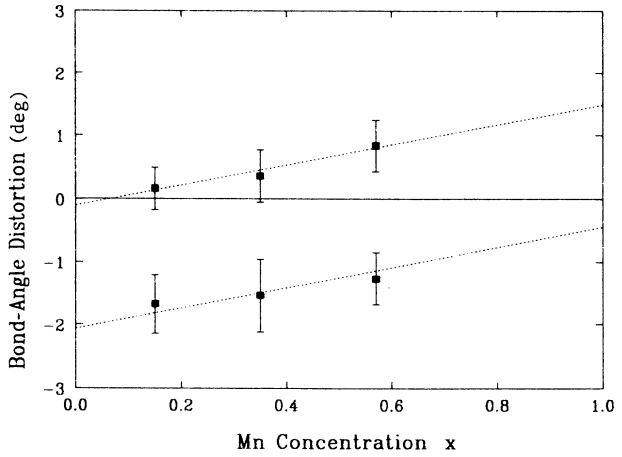

FIG. 14. The amount of the distortion of the tetrahedral cation—Se—cation bond angle $\Delta\theta_{cation\text{-}Se\text{-}cation}$ relative to the ideal value $\theta = 109.6°$. The upper solid squares represent $\Delta\theta_{Zn\text{-}Se\text{-}Zn}$ and the lower solid squares represent $\Delta\theta_{Mn\text{-}Se\text{-}Mn}$. The dashed lines represent the best-fit lines for both Zn and Mn data results, respectively.

$\Delta\theta_{\text{Mn-Se-Mn}}$ is $\sim -1.4°$ at room temperature, in $Zn_{1-x}Mn_xSe$ alloys, which compares fairly well to our extrapolated value at $x=0$ of $\sim -2.0°$ at 77 K. Although they do not mention the possibility of J_{dd} being specifically x dependent, Spalek *et al.* do discuss the fact that their experimental results showed a deviation of the Curie-Weiss temperature $\Theta(T)$ [$\Theta(T)$ is associated with the exchange integral] in $Cd_{1-x}Mn_xTe$ from a constant variation with x, particularly when x is ≥ 0.2, implying that the superexchange integral is dependent on x. Recently, Tsai *et al.*[20] have developed the theoretical framework to explain the nonlinear x dependence of the Curie constant $C(x)$, in terms of the atomic spin value $S(x)$ for the Mn^{2+} ion, for $Cd_{1-x}Mn_xTe$ DMS alloys. Since, according to Spalek *et al.*,[18] the exchange integral J is proportional to $\Theta(T,x)/[S(x)(S(x)+1)]$, we should in principle be able to write an expression for the x dependence of J once the appropriate parameters describing the x dependence of $\Theta(T,x)$ and $S(x)$ are known for $Zn_{1-x}Mn_xSe$. While previous inelastic neutron scattering studies[21] showed the exchange integral J in $Zn_{1-x}Mn_xC^{VI}$(C^{VI}=S,Se,Te) to be essentially independent of Mn concentration in the dilute limit ($x \leq 0.05$), recent studies[22] which covered an extensive range of Mn content show, for $Zn_{1-x}Mn_xTe$ and $Cd_{1-x}Mn_xTe$, that J is indeed x dependent. Also, in a recent study by Larson *et al.*[23] the authors in effect predict that J *does* depend on x.

Results regarding the distribution of Mn^{2+} ions on the cation sublattice in DMS have, prior to this study, been obtained in an indirect way. Although early experimental magnetic susceptibility studies done by Nagata *et al.*[24] were interpreted to show evidence for clustering, later studies[25–28] have supported the notion that the magnetic Mn^{2+} ions in DMS alloys tend to be randomly distributed rather than cluster on the cation sublattice. Our results for the Zn-Mn and Zn-Zn coordination numbers in $Zn_{1-x}Mn_xSe$ show a small but consistent deviation from the random second-shell distribution. However, because the deviation is towards smaller rather than larger Zn-Zn coordination numbers, we conclude that we may have evidence for a tendency for ordering rather than clustering in these alloys.

V. SUMMARY

In conclusion, we have shown that the NN Zn—Se, Mn—Se bond lengths in $Zn_{1-x}Mn_xSe$ remain essentially constant as a function of Mn concentration even though the mean cation-cation distance varies linearly with x throughout the series. This implies a distortion of the crystal structure away from the VCA. While the Se sublattice shows most of the distortion, the cation sublattice also exhibits a moderate amount of relaxation which we believe has to be taken into account in any detailed microstructural model of $Zn_{1-x}Mn_xSe$. The Debye-Waller factors for the NN bond lengths in $Zn_{1-x}Mn_xSe$ are larger for the $x=0.35$ sample, whose concentration lies in the structural phase transition region centered near $x=0.3$, which in our opinion is due to a larger static disorder in the vicinity of the phase transition. We have discovered evidence, based on the observed linear x dependence of the Mn^{2+}—Se^{2-}—Mn^{2+} tetrahedral bond angle, for the antiferromagnetic superexchange integral J_{dd} being x dependent in the range $0.15 \leq x \leq 0.57$. Based on our results, we do not see evidence for the cations, in our $Zn_{1-x}Mn_xSe$ samples, to preferentially cluster but to rather show a slight tendency for ordering.

Note added in proof. With regard to comments made in the present paper on the detailed description of local structure of $Zn_{1-x}Mn_xSe$ and similar alloys requiring a full incorporation of bond bending, bond stretching, and longer-range forces, Weidmann *et al.*[29] have made strain energy calculations for $Zn_{1-x}Mn_xSe$ alloys having a random Mn ion distribution, based on the work first initiated by Gregg and Newman[30] which utilized a modified valence force-field approach, from which they have obtained NNN distances in good agreement with our experimental results.

ACKNOWLEDGMENTS

We thank Dr. T. Elam and Dr. S. Qadri for low-temperature x-ray diffraction measurements. This work was supported in part by the U.S. Office of Naval Research (ONR), under Contract No. N00014-89-J-1108 and by U.S. Defense Advanced Projects Agency (DARPA), under Contract No. N00014-86-K-0760. We also gratefully acknowledge the support of the U.S. Department of Energy (DOE), Division of Materials Research, Office of Basic Energy Sciences under Contract No. DE-FG05-89ER45384 for its role in the development and operation of the X-11 beam line at the National Synchrotron Light Source. The NSLS is supported by the Department of Energy (Divisions of Materials Sciences and Division of Chemical Sciences of the Office of Basic Energy Sciences), under Contract No. DE-AC02-76CD00016.

[1]See, for example, *Diluted Magnetic Semiconductors*, edited by R. L. Aggarwal, J. K. Furdyna, and S. von Molnar (Materials Research Society, Pittsburgh, 1987), Vol. 89; *Semiconductors and Semimetals*, edited by J. K. Furdyna and J. Kossut (Academic, New York, 1988), Vol. 25.

[2]J. K. Furdyna, J. Appl. Phys. **53**, 7637 (1982).

[3]D. R. Yoder-Short, U. Debska, and J. K. Furdyna, J. Appl. Phys. **58**, 4056 (1985).

[4]J. Azoulay, E. A. Stern, D. Shaltiel, and A. Grayevski, Phys. Rev. B **25**, 5627 (1982).

[5]J. C. Mikkelsen, Jr. and J. B. Boyce, Phys. Rev. Lett. **49**, 1412 (1982); Phys. Rev. B **28**, 7130 (1983).

[6]A. Balzarotti, M. Czyzyk, A. Kisiel, N. Motta, M. Podgorny, and M. Zimnal-Starnawska, Phys. Rev. B **30**, 2295 (1984); A. Balzorotti, N. Motta, A. Kisiel, M. Zimnal-Starnawska, M. T. Czyzyk, and M. Podgorny, *ibid.* **31**, 7526 (1985).

[7]Q. Islam and B. A. Bunker, Phys. Rev. Lett. **59**, 2701 (1987).

[8]Hiroyuki Oyanagi, Yoshikazu Takeda, Tadashi Matsushita, Takehiko Ishiguro, and Akio Sasaki, J. Phys. (Paris) Colloq. **47**, C8-423 (1986).

[9]S. M. Islam and B. A. Bunker (unpublished).
[10]U. Debska, W. Giriat, H. R. Harrison, and D. R. Yoder-Short, J. Cryst. Growth **70**, 399 (1984).
[11]D. E. Sayers and B. A. Bunder, in *Extended X-ray Absorption Fine Structure,* edited by D. C. Koningsberger and R. Prins (Wiley, New York, 1988), Chap. 6.
[12]B. K. Teo and P. A. Lee, J. Am. Chem. Soc. **101**, 2815 (1979).
[13]R. A. Mayanovic, W. F. Pong, and B. A. Bunker (unpublished).
[14]W. L. Bragg, Philos. Mag. **40**, 169 (1920); L. Pauling, *The Nature of the Chemical Bond* (Cornell University Press, Ithaca, NY, 1967).
[15]R. A. Mayanovic, W.-F. Pong, and B. A. Bunker (unpublished).
[16]S. M. Durbin (unpublished).
[17]B. E. Larson, K. C. Hass, H. Ehrenreich, and A. E. Carlsson, Solid State Commun. **56**, 347 (1985).
[18]J. Spalek, A. Lewicki, Z. Tarnawski, J. K. Furdyna, R. R. Galazka, and Z. Obuszko, Phys. Rev. B **33**, 3407 (1986).
[19]Way-Faung Pong, Robert A. Mayanovic, and Bruce A. Bunker, Physica B+C **158B**, 617 (1989).
[20]M.-H. Tsai, John D. Dow, R. V. Kasowski, A. Wall, and A. Franciosi, Solid State Commun. **69**, 1131 (1989).
[21]T. M. Giebultowicz, J. J. Rhyne, and J. K. Furdyna, J. Appl. Phys. **61**, 3537 (1987).
[22]T. M. Giebultowicz, J. J. Rhyne, W. Y. Ching, D. L. Huber, J. K. Furdyna, B. Lebech, and R. R. Galazka, Phys. Rev. B **39**, 6857 (1989).
[23]B. E. Larson, K. C. Hass, H. Ehrenreich, and A. E. Carlsson, Phys. Rev. B **37**, 4137 (1988).
[24]Shoichi Nagata, R. R. Galazka, D. P. Mullin, H. Akbarzadeh, G. D. Khattak, J. K. Furdyna, and P. H. Keesom, Phys. Rev. B **22**, 3331 (1980).
[25]Y. Shapira, S. Foner, D. H. Ridgley, K. Dwight, and A. Wold, Phys. Rev. B **30**, 4021 (1984).
[26]Y. Shapira, S. Foner, P. Becla, D. H. Domingues, M. J. Naughton, and J. S. Brooks, Phys. Rev. B **33**, 356 (1986).
[27]R. L. Aggarwal, S. N. Jasperson, P. Becla, and R. R. Galazka, Phys. Rev. B **32**, 5132 (1985).
[28]B. E. Larson, K. C. Hass, and R. L. Aggarwal, Phys. Rev. B **33**, 1789 (1986).
[29]M. R. Weidmann, J. R. Gregg, and K. E. Newman (unpublished).
[30]J. R. Gregg and K. E. Newman, Bull. Am. Phys. Soc. **34**, 592 (1989).

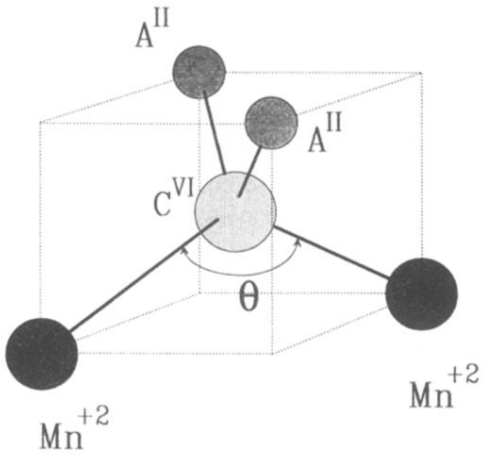

FIG. 13. Schematic of the distorted tetrahedral coordination about a Se atom, showing the bond angle θ. The magnetic interaction between the Mn^{2+} NNN is sensitive to this bond angle.